CRN STRASBOURG

CRN-PN/ 88-37

TWO-PROTON TRANSFER REACTIONS ON EVEN Ni AND Zn ISOTOPES

A. Boucenna, L. Kraus, I. Linck
Centre de Recherches Nucléaires et Université Louis Pasteur, Strasbourg, France
Tsan Ung Chan
Institut des Sciences Nucléaires, Grenoble, France

Submitted for publication in Physical Review C

CENTRE DE RECHERCHES NUCLEAIRES

STRASBOURG

IN2P3 CNRS

UNIVERSITE LOUIS PASTEUR

CRN-PN / 88-37
Submitted to Phys. Rev. C

Two-proton transfer reactions on even Ni and Zn isotopes

A. Boucenna,* L. Kraus, I. Linck
Centre de Recherches Nucléaires, F-67037 Strasbourg Cedex, France

Tsan Ung Chan
Institut des Sciences Nucléaires, F-38026 Grenoble Cedex, France

Two-proton transfer reactions induced by 112 MeV ^{12}C ions on even Ni and Zn isotopes are found to be less selective than the analogous two-neutron transfer reactions induced on the same targets in a similar incident energy range. The additional collective aspects observed in the proton transfer are examined in terms of a semiphenomenological model of two quasi-particles coupled to a triaxial asymmetric rotor. Tentative spin and parity assignments emerge from this comparison, from crude shell model calculations and from systematic trends.

PACS numbers: 25.70.Cd, 27.50.+e, 24.50.+g

I. INTRODUCTION

Most of the high spin states[1] in f-p shell nuclei have been observed by in-beam spectroscopy using fusion-evaporation reactions. These reactions feed only yrast or quasi-yrast states that can have many different configurations. On the other hand, transfer reactions are very selective and favor the population of states with a particular configuration.[2-7] The comparison of results from these two kinds of reactions for the same residual nucleus can shed light on the assignment of J^{π} and/or the level configurations.

Obviously the $g_{9/2}$ shell plays an important role in the explanation of high spin states in the heaviest f-p nuclei,[5,6,8] but due to the large size of the involved matrix complete shell model calculations are scarce. The crude shell model[9] which considers two nucleons moving around an inert target core predicts the energy of high spin states formed by two nucleon transfers as the sum of the excitation energies of the corresponding single particle levels plus (when the two transferred nucleons are identical) an easily calculable pairing energy. Thus the 7^- and 8^+ yrast states in the even isotopes of Zn and Ge have been established as 2n-states.[9] Similarly, the results of $(\alpha, ^2He)$ reaction studies[5,6] on Fe, Ni, Zn and Ge isotopes concord with the predictions of the CSM.[9,10]

The 7^- and 8^+ two-proton high spin states, unobserved up to now, are expected in these nuclei above the similar 2n- configuration states.[10] In order to reach these states, we have performed $(^{12}C, ^{10}Be)$ reactions on Ni and Zn isotopes. Among the residual nuclei studied, ^{66}Zn is of particular interest since it can be formed with 2n and 2p transfer reactions on ^{64}Zn and ^{64}Ni targets respectively. The relative population of states in both reactions will help to distinguish between 2n and 2p states.

Population of states appears less selective in the $(^{12}C, ^{10}Be)$ 2p-transfer reactions than in the 2n-transfers. The interpretation of this observation requires in addition to the 2p cluster selection rules[11] and the CSM predictions,[10] a more sophisticated semi-phenomenological model[12] which considers the coupling of two quasi-particles to a triaxial Davidov rotor in a space including N = 4 $g_{9/2}$ neutron and proton levels.

II. EXPERIMENTAL PROCEDURE

A beam of 112 MeV $^{12}C^{6+}$ was provided by the Strasbourg MP accelerator. Typical beam currents were 50 electrical nA. Targets consisted of self-supporting Ni foils between 80 and 180 $\mu g/cm^2$ thick, and Zn foils between 85 and 228 $\mu g/cm^2$ thick on 20 $\mu g/cm^2$ C backings. These thicknesses have been determined to about 10% with an α-particle gauge. The isotopic enrichments of the $^{58,60,62,64}Ni$ were 99.89%, 99%, 97.94%, 98.02% and of the $^{64,66,68}Zn$ 99.4%, 99%, 98.9% respectively.

Ejectiles were momentum analyzed in a 5 or 10 msr solid angle with the Q3D spectrometer ($dp/p = 2.10^{-4}$) coupled to the incident beam in an energy loss mode. A gaseous hybrid counter composed of three proportional counters separated by two ionization chambers of 4 and 15 cm depth was placed along the focal plane at an angle of 45° to the propagation direction of the detected particles. Two 13 μm mylar foils separated the isobutane of the counter (100 to 150 Torr) from the vacuum of the detection chamber while allowing the particles to reach a 2 cm thick NE110 scintillator.

The ejectiles, detected in the 11% momentum acceptance of the counter, were identified by their energy loss ΔE in the ionization chambers and their residual energy E_R in the scintillator. Correction of the ΔE spectra for entrance angle in the 6° opening of the spectrometer resulted in good mass separation of the detected ejectiles. Position spectra in the first and third proportional counters, separated by 211.5 mm, were obtained by charge division. Conditioned by the ΔE and E_R requirements, the positions allowed reconstruction of the trajectories of the studied ejectiles, the determination of the particle entrance angle, and construction of momentum spectra on the focal plane. The overall energy resolution was 100-200 keV.

III. EXPERIMENTAL RESULTS

The ^{66}Zn spectrum obtained by 2p-transfer (Fig. 1) differs from that of the 2n-transfer spectrum (Fig. 2) in that it shows a larger number of peaks superimposed on a more important background. The selectivity of the 2n-reaction is well explained by the predominant excitation of the configurations $(\nu f_{5/2}\nu g_{9/2})_{7^-}$, $(\nu g_{9/2})^2_{8^+}$ and $(\nu g_{9/2}\nu 2d_{5/2})_{6^+}$ as shown by Jahn[6] with the $(\alpha,^2He)$ reaction. The yet not reported peak at 6.25 MeV could correspond to the $(\nu 2d_{5/2})^2_{4^+}$ configuration calculated with the CSM to lie at 5.819 MeV. The same predominance of the

$(\pi f_{5/2}\pi g_{9/2})_{7^-}$, $(\pi g_{9/2})^2_{8^+}$ and $(\pi g_{9/2}\pi 2d_{5/2})_{6^-}$ stretched natural parity configurations, predicted at 5.119, 6.535 and 7.374 MeV respectively, was expected for the 2p-spectrum.[10] While the peaks at 5.20, 6.85 and 7.55 MeV are good candidates for these states, there are several other strong peaks also, some corresponding to known states.[13] Indeed, in the 2p-transfer case the $2p_{3/2}$, $2p_{1/2}$ and $f_{5/2}$ shells are all available. The filling of these shells leads to configurations of final spin 3^-, 4^+, 5^- and could explain the fact that the peaks from the 3^-, 4^+ and 5^- levels at 2.84, 3.06 and 3.74 MeV respectively are strongly excited in the $^{64}Ni(^{12}C,^{10}Be)^{66}Zn$ reaction but not, or weakly, in $^{64}Zn(^{12}C,^{10}C)^{66}Zn$. In particular, the 5^- state (seen in γ-ray spectroscopy) probably has large $(\pi p_{3/2}\pi g_{9/2})_{5^-}$ and /or $(\pi p_{1/2}\pi g_{9/2})_{5^-}$ components. Two peaks corresponding to energies close to those of 2n-states, i.e. the 4.20 MeV 7^- yrast state and the 5.25 MeV state, previously ascribed $(\nu f_{5/2}\nu g_{9/2})_{7^-}$ and $(\nu g_{9/2})^2_{8^+}$, are surprisingly also well excited in the 2p-transfer. This argues for 2p-components in these states also.

The same considerations hold for the $^{60,62,64}Zn$ (Fig. 3) and the $^{66,68,70}Ge$ spectra (Fig. 4) which appear the less selective as the number of neutrons increases. This is contrary to what is observed in the 2n-transfer spectra on $^{60,62,64,66}Ni$ (Fig. 5).

The greater neutron number (2 to 10) outside the closed $1f_{7/2}$ shell probably contributes to the loss of selectivity of the 2p-transfer reactions on the even Ni and Zn isotopes while the reduced proton number (0 to 2) outside the closed $1f_{7/2}$ shell is of no consequence for the same targets in the 2n-transfer spectra (Fig. 5) in which the $(\nu 2p_{1/2}\,\nu g_{9/2})_{5^-}$, $(\nu f_{5/2}\nu g_{9/2})_{7^-}$, $(\nu f_{5/2}\nu 2d_{5/2})_{5^-}$, $(\nu g_{9/2})^2_{8^+}$ and $(\nu g_{9/2}\nu 2d_{5/2})_{6^-}$ configurations dominate.[6]

The background, which increases with the Q-value of the reaction is more important in the 2p-transfer spectra ($Q(2p) = -27.19$ MeV compared with $Q(2n) = -31.84$ MeV) and adds to the difficulty of their interpretation. In Tables I-VII the experimental excitation energies, given with a precision of 50 keV, are compared with previously known levels for $^{60,64,62,66}Zn$ and $^{70,68,66}Ge$ nuclei, and absolute differential cross-sections are given. These latter have been determined to about 30% and, depending on the transition and on the target range for the well fed transitions, range from 20-500 μb sr for 2p-transfer on Ni isotopes, 100-600 μb/sr for 2p-transfer on Zn isotopes and 60-300 μb/sr for 2n-transfer on Ni isotopes. The 2n values have to be compared with $(\alpha,^2He)$ cross-sections, namely about 50 μb/sr for transitions to the preferentially populated final states.[6] Angular distributions in

1° slices have been obtained over the 6° aperture of the spectrometer. Their shape is not typical enough to serve as a J^π signature.

IV. ANALYSIS

The analysis of the 2p-transfer spectra producing Zn (Fig. 3) and Ge (Fig. 4) isotopes has been made using previously known energy and J^π data (Tables I-VII) and the following considerations.

A. 2p-aspects

In transfer reactions of a (T=1, S=0) 2p-cluster, final states are of natural parity. Kinematical conditions[36] of the present experiment favor L = 6-8$\hbar$ cluster momentum transfers to the final nuclei.[11] Therefore $J^+ = 6^+$, 7^- and 8^+ states should be well populated.

In the simple shell model picture[9,10] this corresponds to the favored filling of the $f_{5/2}$, $g_{9/2}$, and $2d_{5/2}$ shells by two protons moving around an inert target core. The expected positions of the aligned configuration high spin states corresponding to the filling of the available empty shells of the target nuclei have been calculated from recent mass values[37] and single particle energies of Table VIII and are reported in Tables I-VII (CSM column).

B. Collective aspects

Some of the levels excited in the present work are known to belong to positive and negative parity bands. In fact, previous experimental work has shown that prominent features of Zn and Ge spectra are three close-lying $J^\pi = 8^+$ which are qualitatively explained by an 8^+ of the ground state band and the alignment of a proton and a neutron $g_{9/2}$ pair, several negative parity bands, and a γ-band. A recent semi-phenomenological model,[12] gives a quantitative explanation of these characteristics in $^{64,66}Zn$ and $^{64,66,68,70}Ge$.

In this model a pair of quasi-particles of angular momentum J is coupled to an asymmetric triaxial rotor core of angular momentum R to form a state of total angular momentum I. For the positive-parity states both particles are in the $g_{9/2}$ single-particle orbital, and for the negative-parity states one nucleon is in $g_{9/2}$,

while the other is in a $2p_{3/2}$, $2p_{1/2}$ or $1f_{5/2}$ orbital. Amplitude mixing in the wave-functions is explicitly given for ^{68}Ge and ^{66}Ge. The lowest 8^+ state characterized by R (= I) only, corresponds to the ground state rotational band (97.2 % of the wave-function for ^{68}Ge). The second 8^- state contains an aligned neutron pair $\nu_1^2 = (\nu g_{9/2})^2_{J^\pi=8^+}$ and rotations from the core with a kinematical moment R = 0 and R = 2 (64% and 20% respectively of the wave-function for ^{68}Ge). The third band (ν_2^2) corresponds to two $g_{9/2}$ neutrons coupled to 6^- with the core. Petrovici and Faessler[12] predict an 8^- state formed by two aligned protons $(\pi g_{9/2})^2_{J^\pi=8^+}$ at higher energies, or for ^{68}Ge about 1 MeV higher than the third 8^- state.

While the 3^- level is almost an equal admixture of $(\pi p_{3/2}\pi g_{9/2})_{3^-}$ R = 0 and $(\nu p_{3/2}\nu g_{9/2})_{3^-}$ R = 0 configurations, two favored negative parity bands NP1 and NP2 with total angular momentum I = J − R are at higher spins characterized by $(\nu g_{9/2}\nu f_{5/2})_{J=7}$ and $(\pi g_{9/2}\pi f_{5/2})_{J=7}$. NP3 is an unfavored negative parity band characterized with I = R + J -1 and $(\nu g_{9/2}\nu f_{5/2})_{J=7}$ at higher spins.

In Tables I-VII are reported the J^π proposed on the basis of previous data, systematic spectral trends (S) among even isotopes, shell model calculations of two-particle configurations (CSM) and results of the Petrovici-Faessler model. States related by E2 transitions in the referenced γ-ray scheme are indicated in the tables by GS and NP for ground-state positive and negative parity bands respectively.

V. DISCUSSION

In each of Tables I-VII appear one positive parity (GS) and one negative parity band which could be associated with the ground state rotational (GSRB) and one of the negative parity bands of Petrovici and Faessler.[12]

The ground state band previously known up to 6^+ in $^{62,64,66}Zn$ and $^{66,68,70}Ge$ is excited weakly in the corresponding spectra. In ^{70}Zn the γ-ray scheme is not well known.[23] The probable doublet peak observed at 4.40 MeV could contain the 6^+ ground state band member, if it follows the trend in the location of the 6^+ states in the other nuclei. There is a transition reported[20] between a 4.200 MeV state and the 4^+ 2.193 MeV state.

Of the three 8^+ branches in forks reported in some of Zn and Ge isotopes there subsists only one 8^+ state in our spectra, very close to the calculated position of the $(\nu g_{9/2})^2_{8^+}$ configuration. In ^{68}Ge where the triple forking was first observed,[44] the nature of the 8^+ states at 4.837, 5.050 and 5.367 MeV differs according to several interpretations.[12,32,45]. Recent g-factor measurements[33] order them as ν_1^2, ν_2^2 and

GSRB states. This does not agree with the order calculated by Petrovici and Faessler[12] and lends support to the importance of the neutrons of the target outside the closed $f_{7/2}$ shell, as mentioned in Sec. III. This leads us to propose that the peaks at 5.50 MeV in ^{66}Ge and 5.20 MeV in ^{66}Zn are 8^- levels of the same $(\nu_{9/2})^2$ configuration. The same assumption for peaks at 5.70 MeV in ^{64}Zn and 6.30 MeV in ^{62}Zn is more questionable because the correspondence with the calculated energy is less good and the collectivity effect is expected to decrease with the neutron number.

Calculation of the energy of the $(\nu g_{9/2})^2_{8^+}$ configuration in ^{60}Zn requires the position of the $g_{9/2}$ single-particle state in ^{59}Zn which is yet unknown.[38] A level seen at 2.68 MeV in the $^{58}Ni(p,\pi^-)^{59}Zn$ reaction[46] is a possible candidate and would lead to a $(\nu g_{9/2})^2_{8^+}$ excitation energy of 7.24 MeV which is close to the 6.95 MeV peak in ^{60}Zn that systematics indicates as an 8^+ state.

Three strong peaks observed in the ^{66}Zn and $^{70,68}Ge$ spectra belong to a known negative parity band (see Tables I, V and VI). Respectively, the 3^- members are at 2.84, 2.66 and 2.55 MeV, while the 5^- members are at 3.74, 3.67 and 3.50 MeV (not resolved in our spectra from the 6^- GSRB-member in the two last cases) and the 7^- members are at 4.20 MeV (also mixed with the 6^+ GSRB-member), 4.08 and 4.02 MeV. In the isotones ^{64}Zn and ^{66}Ge (see Tables II and VII) the 3^-, 5^-, 7^- members of the same band are reported at 2.998, 3.925, 4.635 MeV and at (2.799), 3.685, 4.207 MeV, respectively. All these states correspond to intense peaks in our spectra except the 5^- members which are weakly excited. The agreement between the location of the 7^- members, and the calculated energy of the $(\nu f_{5/2}\nu g_{9/2})_{7^-}$ configuration as well as the apparent dependence of the relative yields on the neutron number of the target nuclei lead us to propose that we excite the negative-parity band NP1 of Petrovici and Faessler[12] which is composed of mixed neutron and proton configurations for lower spins, and levels of mainly $(\nu f_{5/2}\nu g_{9/2})_{J=7}$ I=J+R nature for higher spins.

A second negative parity band NP2 built on a 5^- state is predicted[12] a little higher in energy with a main configuration $(\pi f_{5/2}\pi g_{9/2})_{J=7}$ I=J+R. In fact, the calculated energies of the high spin stretched 2p- states, which are expected to be strongly excited, correspond to those of the remaining strong spectral peaks. However, few of these states were previously J^π assigned or even known (see Tables I-VII). We propose 4^- as J^π for the 3.71 MeV or 3.82 MeV state in ^{60}Zn and the 3.06 MeV state in ^{66}Ge, because these levels are close to the calculated energy of the $(\pi f_{5/2})^2_{4^-}$ configuration and also in agreement with the systematic trend.

The $(\pi p_{3/2}\pi g_{9/2})_{5^-}$ configuration compatible with all the previous assignments (see Tables I-VII) is often close in energy to the 5^- member of the NP1 band, and in some cases, it is difficult to distinguish between them. In ^{64}Zn and $^{66,70}Ge$ where the NP1 member corresponds to the lowest reported 5^- state, we attribute on yield arguments the $(\pi p_{3/2}\pi g_{9/2})_{5^-}$ configuration to the 4.156 MeV, 3.830 MeV $(3^-,5^-)$ and 3.568 MeV $(2^- - 6^-)$ states, respectively. In ^{68}Ge two 5^- states are reported at 3.582 and 3.650 MeV, but are not distinguishable in our spectrum. Due to the systematic trends and the relative γ-ray decay rate[33] of the 4.054 MeV, 7^- NP1 - member to the 3.582 MeV, 5^- state (52%) and the 3.650 MeV, 5^- state (31%), we argue that the 5^- NP1 - member is at 3.582 MeV and that the 3.650 MeV, 5^- state is mainly of a $(\pi p_{3/2}\pi g_{9/2})_{5^-}$ configuration. The same configuration could explain the important peaks at 4.40 MeV previously J assigned (2 - 6) in ^{60}Zn, at 4.17 MeV in ^{62}Zn and 3.74 MeV in ^{66}Zn.

For all the considered nuclei there exist peaks in the vicinity of the predicted values for the $(\pi f_{5/2}\pi g_{9/2})_{7^-}$, $(\pi g_{9/2})^2_{8^+}$ and $(\pi d_{5/2}\pi g_{9/2})_{6^+}$ configurations (see Tables I-VII). The J^π values of the present work are propositions which could not be checked by partial angular distribution data. A reported (7^-) state at 4.30 MeV in ^{70}Ge reinforces our proposition for the 4.33 MeV peak (Fig. 4).

Table IX gives the comparison of experimental values and CSM predictions for the 7^-, 8^+ and 6^+ 2p-states.

VI. CONCLUSION

The present study of the $(^{12}C,^{10}Be)$ 2p-transfer reactions with 112 MeV ^{12}C on Ni and Zn isotopes complements the $(\alpha,^2He)$ 2n-transfer reaction data. It reveals new 2p-levels in the $^{60,62,64,66}Zn$ and $^{66,68,70}Ge$ final nuclei and leads to high spin and parity assignments, that are proposed on systematical trends and crude shell model calculations. However the J^π signature is not as definite as in the 2n-case where some stretched levels can be unambiguously assigned via angular distribution DWBA fits, which are still meaningful in the $(\alpha,^2He)$ reaction, and correlated with states seen in γ-ray spectroscopy. The $(\pi g_{9/2})^2_{8^+}$ and $(\pi g_{9/2}\pi d_{5/2})_{6^+}$ states predicted to lie a few MeV higher than the corresponding 2n-states are not populated by fusion-evaporation reactions.

The lesser selectivity of the 2p-transfer as compared to the 2n-transfer on the same targets can be related to the greater number of neutrons than protons outside the closed $f_{7/2}$ shell in the target. This fact adds some collectivity to the spectra

that are well explained by the asymmetric rotor model with an admixture of two quasi-particles.[12]

Increasing the incident energy should enhance the selectivity as has been found for 2p-transfers on ^{54}Fe and lighter targets with 40 MeV/nucleon ^{12}C projectiles,[7] and the evolution of the spectra with energy could be interesting. More complete experiments including particle-γ and/or particle-particle angular correlations are needed to check the J^{π} values proposed in the present work and to establish the crude shell model[9] as a valid guide for locating the two-proton stretched states.

ACKNOWLEGMENTS

We thank R. Jahn for sending us a copy of his thesis, and J.A. Cameron for communicating data prior to publication on ^{60}Zn and ^{61}Zn contained in the thesis of D.R. Shubank. Useful discussions with N. Schulz and the critical comments of A. Pape on the manuscript are gratefully acknowledged. We are indebted to F. Jundt and J.C. Sens who participated in the early stages of this work. Thanks are due to the staffs of the MP accelerator and of the Q3D spectrometer for their important assistance. One of us (A.B.) acknowledges the guidance and help of R. Seltz and the financial support from the country of Algeria.

References

* On leave from the University of Setif (Algeria).

1) Table of Isotopes, 7th ed., edited by C.M. Lederer and V.S. Shirley (Wiley, New York, 1978).

2) C.C. Lu, M.S. Zisman, and B.G. Harvey, Phys. Rev. 186, 1086 (1969).

3) N. Anyas-Weiss, J.C. Cornell, P.S. Fisher, P.N. Hudson, A. Menchaca-Rocha, D.J. Millener, A.D. Panagiotou, D.K. Scott, D. Strottman, D.M. Brink, B. Buck, P.J. Ellis, and T. Engeland, Phys. Rep. 12C, 201 (1974).

4) R. Jahn, D.P. Stahel, G.J. Wozniak, R.J. de Meijer, and J. Cerny, Phys. Rev. C 18, 9 (1978).

5) R. Jahn, U. Wienands, D. Wenzel, and P. von Neumann-Cosel, Phys. Lett. 150B, 331 (1985).

6) R. Jahn, Thesis, Institut fur Strahlen- und Kernphysik der Universität Bonn (1985).

7) L. Kraus, A. Boucenna, I. Linck, B. Lott, R.Rebmeister, N. Schulz, J.C. Sens, M.C. Mermaz, B. Berthier, R. Lucas, J. Gastebois, A. Gillibert, A. Miczaika, E. Tomasi-Gustafsson. and C. Grunberg, Phys. Rev. C 37, 2529 (1988).

8 Tsan Ung Chan, J.F. Bruandet, B. Chambon, A. Dauchy, D. Drain, A. Giorni, F. Glasser et C. Morand, Nucl. Phys. A348, 179 (1980).

9) Tsan Ung Chan, M. Agard, J.F. Bruandet, and C. Morand, Phys. Rev. C 19, 244 (1979).

10) Tsan Ung Chan, Phys. Rev. C 36, 838 (1987).

11) A. Boucenna, L. Kraus, I. Linck, B. Lott, R. Rebmeister, N. Schulz, J.C. Sens, A. Abzouzi, B. Berthier, J. Gastebois, A. Gillibert, R. Lucas, M.C. Mermaz, A. Miczaika, E. Tomasi-Gustafsson, and C. Grunberg, XXVI International Meeting on Nuclear Physics, Bormio 25-30 January 1988, p. 441, ed. Iona IORI.

12) A. Petrovici and Amand Faessler, Nucl. Phys. A395, 44 (1983).

13) N.J. Ward and F Kearns, Nucl. Data Sheets, 39, 1 (1983).

14) J. Jabbour, L.H. Rosier, B. Ramstein, R. Tamisier, and P. Avignon, Nucl. Phys. A464, 260 (1987).

15) G.F. Neal, Z.P. Zawa, F.P. Venezia, and P.R. Chagnon, Nucl. Phys. A280, 161 (1977).

16) H.L. Halbert, Nucl. Data Sheets 28, 179 (1979).

17) D.N. Simister, L.P. Ekström, G.D. Jones, F. Kearns, T.P. Morrison, O.M. Mustaffa, H.G. Price, P.J. Twin, R. Wadsworth, and N.J. Ward, J. Phys. G : Nucl. Phys. 6, 81 (1980).

18) H.L. Halbert, Nucl. Data Sheets 26, 5 (1979).

19) Y. Okuma, T. Yanabu, T. Motobayashi, K. Takimoto, S. Mitsuki, K. Ogino, T. Shimoura, M. Fukada, and T. Suehiro, Annual Report RCNP Osaka, p. 92 (1982).

20) G.P.A. Berg, B. Berthier, J.P. Fouan, J. Gastebois, J.P. Le Fèvre, and M.C. Lemaire, Phys. Rev. C 18, 2204 (1978).

21) H. Verheul, Nucl. Data Sheets 13, 443 (1974).

22) A. Watt, R.P. Singhal, M.H. Storm, and R.R. Whitehead, J. Phys. G7, L145 (1981).

23) P. Anderson, L.P. Ekström, and J. Lyttkens, Nucl. Data Sheets 48, 251 (1986).

24) D.J. Weber, G.M. Crawley, W. Benenson, E. Kashy, and H. Nann, Nucl. Phys. A313, 385 (1979).

25) D. Evers, W. Assmann, K. Rudolph, S.J. Skorka, and P. Sperr, Nucl. Phys. A230, 109 (1974).

26) J.A. Cameron, private communication of some elements of the Ph. D. Thesis of R. Schubank, Mc Master University.

27) M.R. Bhat, Nucl. Data Sheets 51, 95 (1987).

28) A.D. Efimov, K.I. Erokhina, V.G. Kiptilyi, I.Kh. Lemberg, V.M. Mikhailov, and B.I. Rzhanov, Izv. Akad. Nauk. SSSR. Ser. Fiz. 48, 10 (1984).

29) L. Cleemann, U. Eberth, J. Eberth, W. Neumann, and V. Zobel, Phys. Rev. C 18, 1049 (1978).

30) M.R. Bhat, Nucl. Data Sheets 55, 1 (1988).

31) T. Paradellis and C.A. Kalfas, Phys. Rev. C 25, 350 (1982).

32) A.P. de Lima, A.V. Ramayya, J.H. Hamilton, B. Van Nooijen, R.M. Ronningen, H. Kawakami, R.B. Piercey, E. de Lima, R.L. Robinson, H.J. Kim, L.K. Peker, F.A. Rickey, R. Popli, A.J. Caffrey, and J.C. Wells, Phys. Rev. C 23, 213 (1981); Erratum Phys. Rev. C 23, 2380 (1981).

33) M.E. Barclay, L. Cleemann, A.V. Ramayya, J.H. Hamilton, C.F. Maguire, M.C. Ma, R. Soundranayagam, K. Zhao, A. Balanda, J.D. Cole, R.B. Piercey, Amand Faessler, and S. Kuyucak, J. Phys. G12, L295 (1986).

34) L. Cleemann, J. Eberth, W. Neumann, N. Wiehl, and V. Zobel, Nucl. Phys. A334, 157 (1980).

35) R. Soundranayagam, R.B. Piercey, A.V. Ramayya, J.H. Hamilton,A.Y. Ahmed, H. Yamada, C.F. Maguire, G.L. Bomar, R.L. Robinson, and H.J. Kim, Phys. Rev. C 25, 1575 (1982).
36) D.M. Brink, Phys. Lett. 40B, 37 (1972).
37) A.H. Wapstra, G. Audi and R. Hoekstra, At. Data Nucl. Data Tables 39, 281 (1988).
38) P. Andersson, L.P. Ekström, and J. Lyttkens, Nucl. Data Sheets 39, 641 (1983).
39) L.P. Ekström and J. Lyttkens, Nucl. Data Sheets 38, 463 (1983).
40) R.L. Auble, Nucl. Data Sheets 28, 559 (1979).
41) N.J. Ward and J.K. Tuli, Nucl. Data Sheets 47, 135 (1986).
42) J.N. Mo and S. Sen, Nucl. Data Sheets 39, 741 (1983).
43) F. Kearns and N.J. Ward, Nucl. Data Sheets 35, 101 (1982).
44) A.P. de Lima, J.H. Hamilton, A V. Ramayya, B. van Nooijen, R. M. Ronningen, H. Kawakami, R.B. Piercey, E. de Lima, R.L. Robinson, H.J. Kim, W.K. Tuttle, L.K. Peker, F.A. Rickey, and R. Popli, Phys. Lett. 83B, 43 (1979).
45) K.J. Weeks, C.S. Han, and J.P. Draayer, Nucl. Phys. A371, 19 (1981).
46) B. Sherril, K. Beard, W. Benenson, B.A. Brown, E. Kashy, W.E. Otrand, H. Nann, J.J. Kahayias, A.D. Bacher, and T.E. Ward, Phys. Rev. C 28, 1712 (1983).
47) J. Görres, T. Chapuran, D.P. Balamuth, and J.W. Arrison, Phys. Rev. Lett. 58, 662 (1987).

TABLE I. Excitation energy, spin and parity of ^{66}Zn levels.

Previous works			Present work					
E_x (MeV)	J^π	Band[d]	E_x (MeV)	$d\sigma/d\omega$[c] (μb/sr)	Configuration	CSM (MeV)	J^π[f]	
0.000[a, b]	0	GS	0.0					
1.039[a, b]	2^+	GS	1.04	73				
1.873[a, b]	2^+		1.89					
2.450[a, b]	4^+	GS	2.47					
2.827[a, b]	3^-	NP	2.84	172				
3.077[a, b]	4^+		3.06	245	$(\pi f_{5/2})^2{}_{4+}$	3.703		
3.746[a]	5^-	NP	3.74	210	$(\pi p_{3/2}\pi g_{9/2})_{5^-}$	4.007		
4.182[a]	(6^+)	GS						
			4.20	292				
4.251[a, c]	(7^-)	NP			$(\nu f_{5/2}\nu g_{9/2})_{7^-}$	4.146	7^-	S
4.814[a]	(7^-)		4.80	125				
					$(\pi f_{5/2}\pi g_{9/2})_{7^-}$	5.122	(7^-)	S,T
5.207[a, c]	(8^+)	GS	5.20	284	$(\nu g_{9/2})^2{}_{8+}$	5.211	8^+	S
5.464[a]	(9^-)	NP	5.40					
			5.60					
5.74[c]	(6^+)							
			6.00					
			6.85	196	$(\pi g_{9/2})^2{}_{8+}$	6.541	(8^+)	S, T
			7.55	180	$(\pi g_{9/2}\pi d_{5/2})_{6+}$	(7.398)	(6^+)	S, T

[a] Ref. 13
[b] Ref. 14
[c] Ref. 6
[d] Ref. 15
[e] Cross section at θ_{lab}= 10° with an absolute error of 30%.
[f] Spin and parity assignments at the right in the table are based on systematic trends (S) and on crude shell model (CSM) calculations (T).

TABLE II. Excitation energy, spin and parity of ^{64}Zn levels.

Previous works			Present work					
E_x (MeV)	J^π	Band[c]	E_x (MeV)	$d\sigma/d\omega$[d] (μb/sr)	Configuration	CSM (MeV)	J^π[e]	
0.000[a, b]	0^+	GS	0.00					
0.991[a, b]	2^+	GS	0.98	76				
1.799[a, b]	2^+		1.80					
2.307[a, b]	4^+	GS	2.40					
2.998[a, b]	3^-	NP	3.06	434				
3.078[a, b]	4^+				$(\pi f_{5/2})^2{}_{4^+}$	3.514		
3.925[a, b]	5^-	NP						
3.993	6^+	GS						
4.156	5^-		4.10	530	$(\pi p_{3/2}\pi g_{9/2})_{5^-}$	4.096		
4.237	6^+							
4.635[a, b]	7^-	NP	4.65	185	$(\nu f_{5/2}g_{9/2})_{7^-}$	4.645		
4.981[a, b]	7^-							
5.151[a]	(6,7)							
			5.30	434	$(\pi f_{5/2}\pi g_{9/2})_{7^-}$	5.058	(7^-)	S, T
5.680[a, c]	$8^{(-)}$, $(9)^-$	NP	5.70	186			(8^+)	S
6.124[a]	(9^-)				$(\nu g_{9/2})^2{}_{8^+}$	6.156		
			6.30					
6.766[a]			6.70	315	$(\pi g_{9/2})^2{}_{8^+}$	6.602	(8^+)	T
			7.40					
			7.90	521	$(\pi g_{9/2}\pi d_{5/2})_{6^+}$	7.572	(6^+)	T[f]

[a] Ref. 16
[b] Ref. 14
[c] Ref. 17

[d] Cross section at $\theta_{lab} = 10°$ with an absolute error of 30%.

[e] Spin and parity assignments at the right in the table are based on systematic trends (S) and on crude shell model (CSM) calculations (T).

[f] The 7.90 MeV peak is choosen as (6^+) rather than the 7.40 MeV one on yield considerations.

TABLE III. Excitation energy, spin and parity of ^{62}Zn levels.

Previous works			Present work					
E_x (MeV)	J^π	Band[e]	E_x (MeV)	$d\sigma/d\omega$[f] (μb/sr)	Configuration	CSM (MeV)	J^π_g	
0.00[a, b]	0^+	GS	0.0					
0.95[a, b]	2^+	GS	0.96	19				
1.81[a,b]	2^+		1.80					
2.19[a, b]	4^+	GS	2.20					
3.20[b, c, e]	(3^-)	NP					3^-	S
			3.31	116				
3.216[d]	(4^+)				$(\pi f_{5/2})_{4^+}$	3.610	4^+	S, T
3.71[e]	6^+	GS						
4.05[b, c]	5^-	NP	4.17	141	$(\pi p_{3/2}\pi g_{9/2})_{5^-}$	4.391		
4.347[e]	6^+							
4.54[b]	6^+		4.50	47				
			4.70		$(\nu f_{5/2}\nu g_{9/2})_{7^-}$	4.795	7^-	S
4.90[a, e]	(7^-)							
5.122[e]	5, 7	NP	5.19	171	$(\pi f_{5/2}\pi g_{9/2})_{7^-}$	5.361	7^-	T
			6.30		$(\nu g_{9/2})^2_{8^+}$	(6.673)	(8^+)	S
					$(\pi g_{9/2})^2_{8^+}$	7.112	(8^+)	T
			7.54	106				
					$(\pi g_{9/2}\pi d_{5/2})_{6^+}$	(7.80)	(6^+)	T

[a] Ref. 18
[b] Ref. 19
[c] Ref. 20
[d] Ref. 21
[e] Ref. 22

[f] Cross section at θ_{lab}= 10° with an absolute error of 30%.

[g] Spin ans parity assignments at the right in the table are based on systematic trends (S) and on crude shell model (CSM) calculations (T).

TABLE IV. Excitation energy, spin and parity of ^{60}Zn levels.

Previous works			Present work					
E_x (MeV)	J^π	Band[d]	E_x (MeV)	$d\sigma/d\omega$[e] (μb/sr)	Configuration	CSM (MeV)	J^π[f]	
0.000[a]	0^+							
1.004[a]	2^+	GS	1.01	3				
2.193[a]	4^+	GS	2.19	3				
3.504[a]	3^-	NP	3.59	10				
			3.71		$(\pi f_{5/2})^2{}_{4^+}$	3.531		
3.82[b, d]	(0-4)		3.84					
4.200[d]		GS					(6^+)	S
4.36[a, b, d]	(2-6)		4.40	30	$(\pi p_{3/2}\pi g_{9/2})_{5^-}$	4.746	(5^-)	T
5.35[a, b]	4^+		5.30	27	$(\nu f_{5/2}\nu g_{9/2})_{7^-}$	(5.45)	(7^-)	S, T
					$(\pi f_{5/2}\pi g_{9/2})_{7^-}$	5.660		
6.63[a, c, d]	(0-4)							
			6.95	16	$(\nu g_{9/2})^2{}_{8^+}$	(7.24)	(8^+)	S
7.38[a, c]			7.35					
7.66[a, b]								
			7.98	8	$(\pi g_{9/2})^2{}_{8^+}$	7.788	(8^+)	T
			8.30	6	$(\pi g_{9/2}\pi d_{5/2})_{6^+}$	8.326	(6^+)	T
8.73[a, c, d]			8.75		$(\pi d_{5/2})^2{}_{4^+}$	8.863	(4^+)	T

[a] Ref. 23
[b] Ref. 24
[c] Ref. 25
[d] Ref. 26

[e] Cross section at θ_{lab}= 10° with an absolute error of 30%.

[f] Spin and parity assignments at the right in the table are based on systematical trends (S) and on crude shell model (CSM) calculations (T).

TABLE V. Excitation energy, spin and parity of ^{70}Ge levels.

Previous works			Present work					
E_x (MeV)	J^π	Band[c]	E_x (MeV)	$d\sigma/d\omega$[d] (μb/sr)	Configuration	CSM (MeV)	J^πe	
0.000[a]	0^+	GS	0.0					
1.039[a]	2^+	GS	1.03	72				
2.153[a]	4^+	GS	2.13					
2.561[a]	3^-	NP	2.55	173				
3.059[a]	4^+		3.05	317	$(\pi f_{5/2})^2_{4+}$	3.071		
3.297[a]	6^+	GS						
			3.50	101				
3.417[a]	5^-	NP						
3.568[a]	$(2^-\text{-}6^-)$				$(\pi p_{3/2}\pi g_{9/2})_{5^-}$	3.893		
3.955[a]	7^-	NP	4.02	220	$(\nu f_{5/2}\nu g_{9/2})_{7^-}$	3.744		
4.202[a]	8^+	GS			$(\nu g_{9/2})^2_{8+}$	(4.142)		
			4.33	591				
4.30[b]	(7^-)				$(\pi f_{5/2}\pi g_{9/2})_{7^-}$	4.467	7^-	T, S
4.430[a]	8^+							
4.984[a]			4.92					
			5.42					
			5.73		$(\pi g_{9/2})^2_{8+}$	5.863	(8^+)	T
			6.60		$(\pi g_{9/2}\pi d_{5/2})_{6+}$	(6.377)	(6^+)	T
			7.04		$(\pi d_{5/2})^2_{4+}$	(6.891)	(4^+)	T

[a] Ref. 27
[b] Ref. 28
[c] Ref. 29
[d] Cross section at θ_{lab}= 10° with an absolute error of 30%.
[e] Spin and parity assignments at the right in the table are based on systematic trends (S) and on crude shell model (CSM) calculations (T).

TABLE VI. Excitation energy, spin and parity of ^{68}Ge levels.

Previous works			Present work					
E_x (MeV)	J^π	Band[d]	E_x (MeV)	$d\sigma/d\omega$[e] (μb/sr)	Configuration	CSM (MeV)	J^π[f]	
0.000[a, b]	0^+	GS	0.0					
1.016[a, b, c]	2^+	GS	1.03	22				
1.778[a, b, c]	2^+		1.80					
2.268[a, b, c]	4^+	GS	2.28					
2.649[a, b]	3^-	NP	2.66	148				
3.041[a]	(4^+)		3.05	116	$(\pi f_{5/2})^2{}_4+$	2.838	4^+	S, T
3.650[c]	5^-	NP	3.67	130	$(\pi p_{3/2}\pi g_{9/2})_5-$	4.194		
3.696[a, c]	6^+	GS						
4.054[c]	7^-	NP	4.08	292	$(\nu f_{5/2}\nu g_{9/2})_7-$	(4.056)		
			4.61	156	$(\pi f_{5/2}\pi g_{9/2})_7-$	4.553	7^-	T
4.837[a,c]	(8^+)	GS	4.81	210	$(\nu g_{9/2})^2{}_8+$	(4.790)	8^+	S
5.151[a]			5.18					
			5.56					
			6.30		$(\pi g_{9/2})^2{}_8+$	6.268	(8^+)	T
			6.96		$(\pi g_{9/2}\pi d_{5/2})_6+$	(6.940)	(6^+)	T

[a] Ref. 30
[b] Ref. 31
[c] Ref. 32
[d] Ref. 33

[e] Cross section at θ_{lab}= 10° with an absolute error of 30%.

[f] Spin and parity assignments at the right in the table are based on systematic trends (S) and on crude shell model (CSM) calculations (T).

TABLE VII. Excitation energy, spin and parity of ^{66}Ge levels.

Previous works			Present work					
E_x (MeV)	J^π	Band[c]	E_x (MeV)	$d\sigma/d\omega$[d] (μb/sr)	Configuration	CSM (MeV)	J^π[e]	
0.000[a,b]	0^+	GS	0.0					
0.957[a,b]	2^+	GS	0.93	1				
2.174[a,b]	4^+	GS	2.17					
2.799[a,c]	(3^-)	NP	2.80	37			3^-	S
3.025[a,c]	$(3^-,5^-)$							
3.080[a]			3.06	11	$(\pi f_{5/2})_{4+}$	2.699	4^+	S, T
3.656[a,b,c]	(6^+)	GS	3.60					
3.685[a,b,c]	5^-	NP						
3.830[a,c]	$(3^-, 5^-)$		3.83	94	$(\pi p_{3/2}\pi g_{9/2})_{5^-}$	4.357	5^-	S,T
3.841[a]								
4.207[a,b,c]	7^-	NP	4.20	83	$(\nu f_{5/2}\nu g_{9/2})_{7^-}$	4.557		
4.544[a,b,c]			4.59	53	$(\pi f_{5/2}\pi g_{9/2})_{7^-}$	4.548	(7^-)	S, T
			4.92	45				
5.495[a,b,c]	$(6\text{-}9)^-$	NP						
			5.50	37	$(\nu g_{9/2})^2{}_{8+}$	5.662	8^+	S
5.534[a]	(8^+)							
6.505[a]								
			6.63	71	$(\pi g_{9/2})^2{}_{8+}$	6.397	(8^+)	T
			7.27	76	$(\pi g_{9/2}\pi d_{5/2})_{6+}$	(7.179)	(6^+)	T

[a] Ref. 13
[b] Ref. 34
[c] Ref. 35

[d] Cross section at θ_{lab}= 10° with an absolute error of 30%.

[e] Spin and parity assignments at the right in the table are based on systematic trends (S) and on crude shell model (CSM) calculations (T).

TABLE VIII.Single particle energies (MeV) used in the crude shell model calculations.

	$2p_{3/2}$	$1f_{5/2}$	$2p_{1/2}$	$1g_{9/2}$	$2d_{5/2}$
^{59}Cu[a]	0.	0.914	0.491	3.043	3.580
^{61}Cu[b]	0.	0.970	0.475	2.721	(3.406)
^{63}Cu[c]	0.	0.962	0.670	2.506	3.476
^{65}Cu[d]	0.	1.115	0.771	2.534	(3.391)
^{65}Ga[d]	0.	0.191	(0.062)	2.040	(2.822)
^{67}Ga[e]	0.	0.359	0.167	2.074	(2.746)
^{69}Ga[f]	0.	0.574	0.319	1.970	(2.484)
^{59}Ni[a]	0.	0.339	0.465	3.055	4.462
^{61}Ni[b]	0.	0.067	0.283	2.122	2.697
^{63}Ni[c]	0.155	0.087	0.	(1.292)	2.297
^{65}Ni[d]	0.692	0.	0.063	1.013	1.920
^{59}Zn[a, g]	0.	(0.90)	(0.54)	(2.68)	
^{61}Zn[b]	0.	0.124	(0.088)	(2.002)	
^{63}Zn[c]	0.	0.193	0.248	1.704	
^{65}Zn[d]	0.115	0.	(0.054)	1.065	1.370
^{65}Ge[h]	0.	0.111		1.216	
^{67}Ge[e]	(0.123)	(0.018)	(0.)	(0.752)	
^{69}Ge[f]	0.233	0.	0.087	(0.398)	

[a] Ref. 38
[b] Ref. 39
[c] Ref. 40
[d] Ref. 41
[e] Ref. 42
[f] Ref. 43
[g] Ref. 46
[h] Ref. 47

TABLE IX. Crude shell model and experimental energies (MeV) of assumed 2p-states in Zn and Ge isotopes.

	$(\pi f_{5/2}\pi g_{9/2})_{7^-}$		$(\pi g_{9/2})^2_{8^+}$		$(\pi g_{9/2}\pi d_{5/2})_{6^+}$		$(d_{5/2})^2_{4^+}$	
^{60}Zn	5.660	5.30	7.788	7.98	8.326	8.30	8.863	8.75
^{62}Zn	5.361	5.19	7.112	7.54	(7.80)	7.54	(8.482)	
^{64}Zn	5.058	5.30	6.602	6.70	7.572	7.90	8.542	
^{66}Zn	5.122	5.20	6.541	6.85	(7.398)	7.55	(8.255)	
^{66}Ge	4.548	4.59	6.397	6.63	7.179	7.27	(7.961)	
^{68}Ge	4.553	4.61	6.268	6.30	6.940	6.96	(7.612)	
^{70}Ge	4.467	4.33	5.863	5.73	(6.377)	6.60	(6.891)	

Figure captions

Fig.1 : The ^{66}Zn spectrum obtained by a 2p-transfer reaction (Q = -10.806 MeV). This is to be compared with the ^{66}Zn spectrum of Fig. 2 obtained in the same conditions by a 2n-transfer reaction (Q = -12.803 MeV).

Fig. 2 : See caption of Fig. 1.

Fig. 3 : Two-proton transfers on $^{58,60,62,64}Ni$. The respective Q-values are -18.647, -15.908, -13.350 and -10.806 MeV.

Fig. 4 : Two-proton transfers on $^{64,66,68}Zn$. The respective Q-values are -16.989, -14.538 and -12.052 MeV.

Fig. 5 : Two-neutron transfers on $^{58,60,62,64}Ni$ The respective Q-values are -11.453, -13.424, -15.347 and -16.768 MeV. The J^{π} values are those deduced from the $(\alpha,^{2}He)$ reactions.[7]

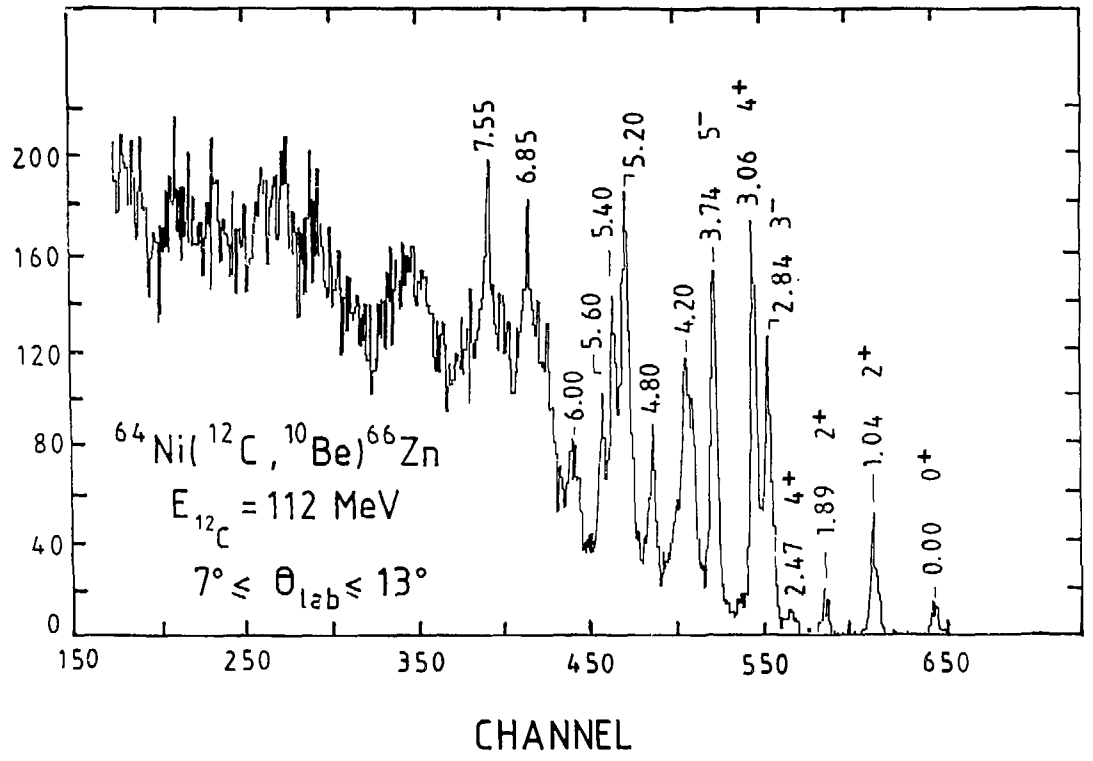
COUNTS
CHANNEL
200
160
120
80
40
0
150
250
350
450
550
650
^{64}Ni(^{12}C, ^{10}Be)^{66}Zn
$E_{^{12}C}$ = 112 MeV
7° ≤ θ_{lab} ≤ 13°
7.55
6.85
6.00
5.60
5.40
5.20
4.80
4.20
3.74
5⁻
3.06
4⁺
3⁻
2.84
2.47
4⁺
1.89
2⁺
1.04
2⁺
0.00
0⁺

Figure 1

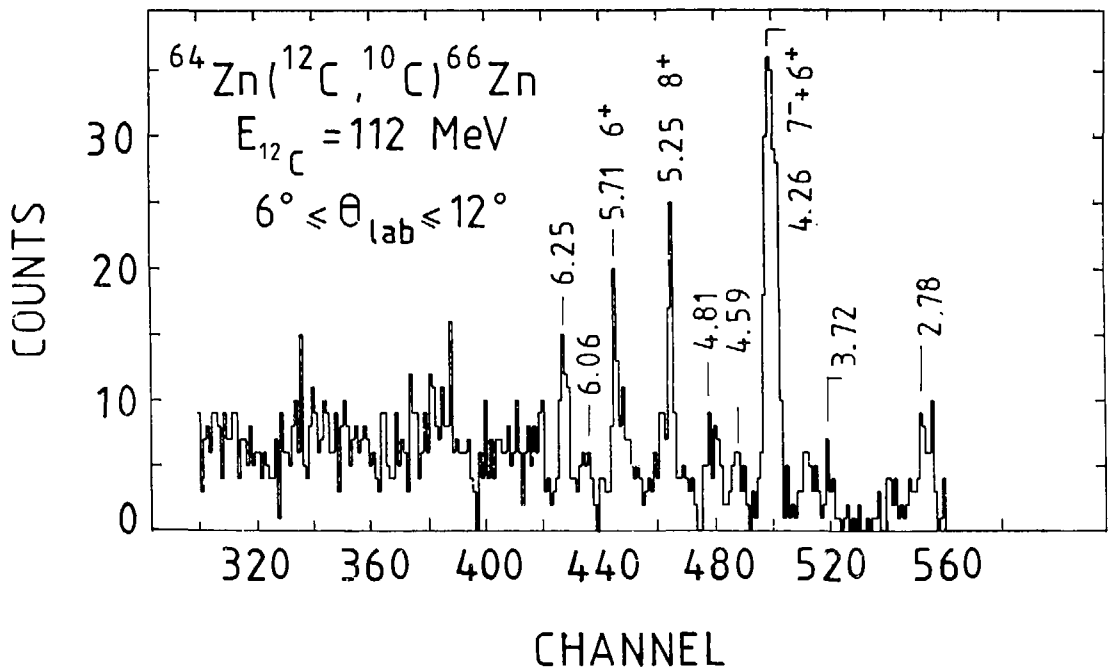
$^{64}Zn(^{12}C, ^{10}C)^{66}Zn$
$E_{^{12}C} = 112$ MeV
$6° \leqslant \theta_{lab} \leqslant 12°$
6.25
6.06
5.71 6+
5.25 8+
4.81
4.59
4.26 7⁻+6+
3.72
2.78
COUNTS
CHANNEL
0
10
20
30
320
360
400
440
480
520
560

Figure 2

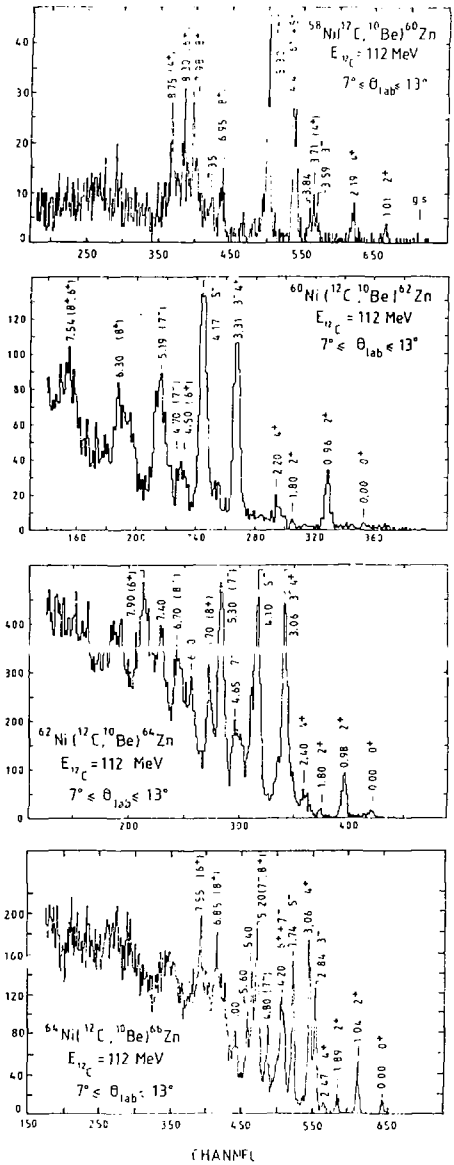
^{58}Ni(^{12}C, ^{10}Be)^{60}Zn
$E_{^{12}C}$ = 112 MeV
7° ≤ θ_{lab} ≤ 13°
^{60}Ni(^{12}C, ^{10}Be)^{62}Zn
$E_{^{12}C}$ = 112 MeV
7° ≤ θ_{lab} ≤ 13°
^{62}Ni(^{12}C, ^{10}Be)^{64}Zn
$E_{^{12}C}$ = 112 MeV
7° ≤ θ_{lab} ≤ 13°
^{64}Ni(^{12}C, ^{10}Be)^{66}Zn
$E_{^{12}C}$ = 112 MeV
7° ≤ θ_{lab} ≤ 13°
COUNTS
CHANNEL

Figure 3

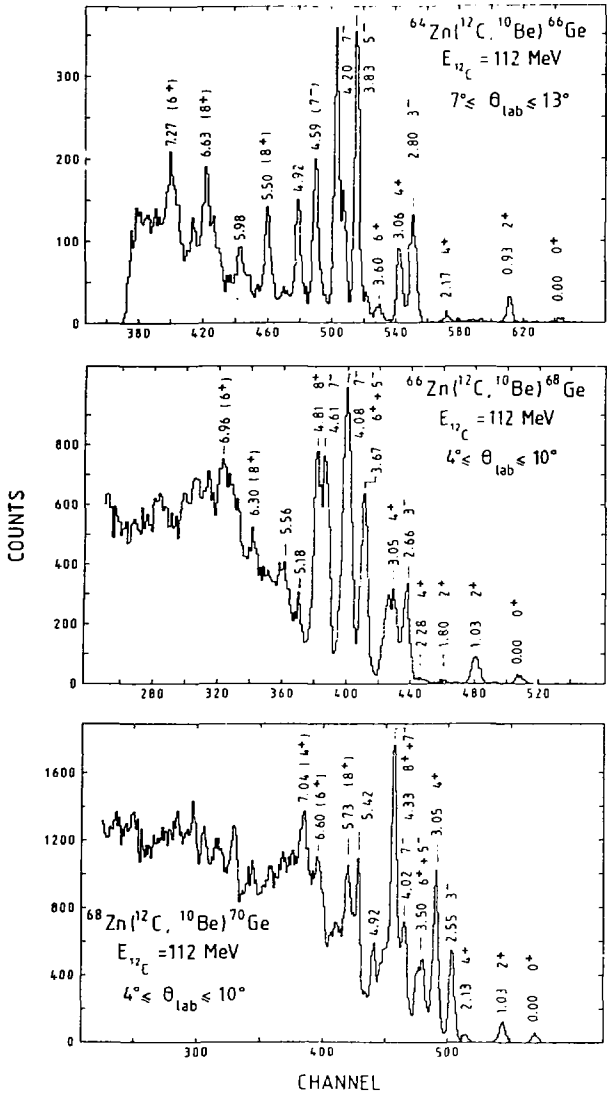
^{64}Zn(^{12}C, ^{10}Be)^{66}Ge
$E_{^{12}C}$ = 112 MeV
7° ≤ θ_{lab} ≤ 13°
7.27 (6+)
6.63 (8+)
5.98
5.50 (8+)
4.92
4.59 (7−)
4.20 7−
3.83 5−
3.60 6+
3.06 4+
2.80 3−
2.17 4+
0.93 2+
0.00 0+
^{66}Zn(^{12}C, ^{10}Be)^{68}Ge
$E_{^{12}C}$ = 112 MeV
4° ≤ θ_{lab} ≤ 10°
6.96 (6+)
6.30 (8+)
5.56
5.18
4.81 8+
4.61 7−
4.08 6+ + 5−
3.67
3.05 4+
2.66 3−
2.28 4+
1.80 2+
1.03 2+
0.00 0+
^{68}Zn(^{12}C, ^{10}Be)^{70}Ge
$E_{^{12}C}$ = 112 MeV
4° ≤ θ_{lab} ≤ 10°
7.04 (4+)
6.60 (6+)
5.73 (8+)
5.42
4.92
4.33 8+ + 7−
4.02 7− + 5−
3.50 6+
3.05 4+
2.55 3−
2.13 4+
1.03 2+
0.00 0+
COUNTS
CHANNEL

Figure 4

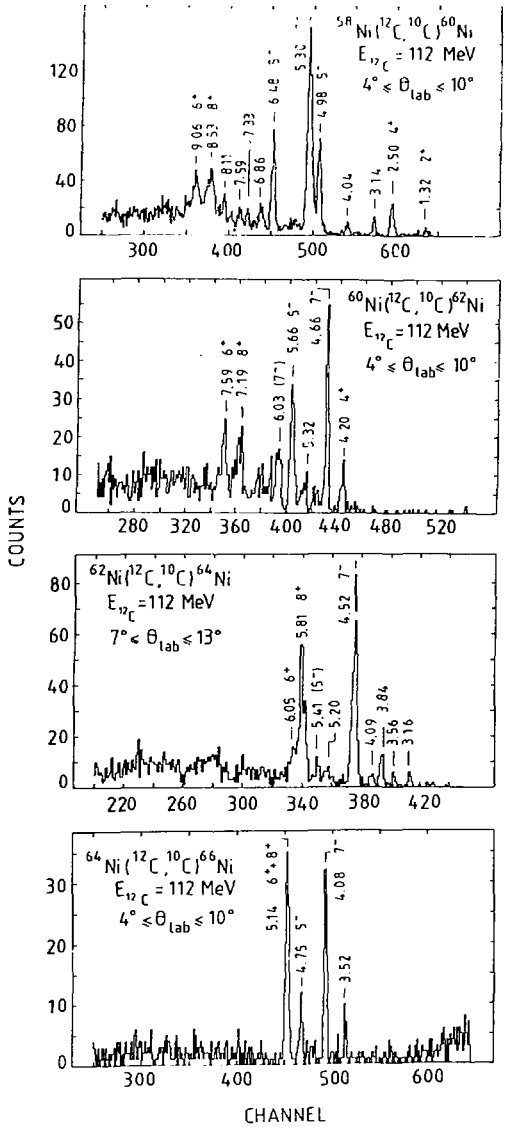
^{58}Ni(^{12}C,^{10}C)^{60}Ni
$E_{^{12}C}$ = 112 MeV
4° ≤ θ_{lab} ≤ 10°
9.06 6⁺
8.53 8⁺
8.11
7.59
7.33
6.86
6.48 5⁻
5.30
4.98 5⁻
4.04
3.14
2.50 4⁺
1.32 2⁺
^{60}Ni(^{12}C,^{10}C)^{62}Ni
$E_{^{12}C}$ = 112 MeV
4° ≤ θ_{lab} ≤ 10°
7.59 6⁺
7.19 8⁺
6.03 (7⁻)
5.66 5⁻
4.66 7⁻
5.32
4.20 4⁺
^{62}Ni(^{12}C,^{10}C)^{64}Ni
$E_{^{12}C}$ = 112 MeV
7° ≤ θ_{lab} ≤ 13°
6.05 6⁺
5.81 8⁺
5.41 (5⁻)
5.20
4.52 7⁻
4.09
3.84
3.56
3.16
^{64}Ni(^{12}C,^{10}C)^{66}Ni
$E_{^{12}C}$ = 112 MeV
4° ≤ θ_{lab} ≤ 10°
5.14 6⁺,8⁺
4.75 5⁻
4.08 7⁻
3.52
COUNTS
CHANNEL

Figure 5